



## DEVELOPMENT OF HYDROXYAPATITE-CHITOSAN BEADS AS A SUSTAINED DRUG DELIVERY SYSTEM TO BONE

Pichatborvonkul P<sup>1</sup>, Kaewsrichan J<sup>\*2</sup> and Kaewsichan L<sup>1</sup>

<sup>1</sup>Department of Chemical Engineering, Faculty of Engineering, Prince of Songkla University,  
Hat-yai, Songkhla, 90112, Thailand

<sup>2</sup>Drug Delivery System Excellence Center, Faculty of Pharmaceutical Sciences,  
Prince of Songkla University, Hat-yai, Songkhla, 90112, Thailand

### ARTICLE INFO

Submitted: 05-01-2012

Accepted: 12-06-2012

\*Corresponding Author: Dr.  
JasadeeKaewsrichan

Email: jasadee.k@psu.ac.th

### KEYWORDS

Hydroxyapatite,  
Chitosan beads,  
Polymer-ceramic hybrid,  
Sustained drug delivery,  
Tissue engineering,  
Drug encapsulation

### ABSTRACT

Composites of natural polymers and ceramics have become important in the development of biomedical applications ranging from diagnostic and therapeutic devices, tissue regeneration and controlled drug delivery. This study explored the potential of hydroxyapatite (HA)/chitosan (CH) composites to act as a sustained drug delivery to bone.

Porous HA/CH composite beads were prepared by ionic cross-linking using tripolyphosphate (TPP). The structure and morphology of beads were investigated by SEM. The polymer-ceramic interactions and polymer cross-linking were examined by FTIR. To encapsulate tetracycline hydrochloride (TCH) in the cross-linked beads, a negatively pressurized system was applied. The degrees of cross-linking and swelling that affected the drug release pattern were determined.

The pore size of the beads ranged between 40 and 100  $\mu\text{m}$ , which negatively dependent on HA content and cross-linking density. The deposition of apatite after submerging the beads in phosphate buffer saline (PBS) pH 7.4 for 7 days indicated their bioactive property. The *in vitro* drug release test demonstrated that the successive and dense HA/CH composite endowed the beads with a sustained drug release pattern without initial burst release.

The high effectiveness of cross-linked CH beads in regulating the release of TCH might be capable to serve as a temporary drug carrier in bone tissue regeneration.

### 1.0 Introduction

Chitosan (CH) is derived from *N*-deacetylation of chitin, which is the second most abundant naturally occurring biopolymer after cellulose.<sup>1</sup> Due to its biodegradable and biocompatible properties, CH has been investigated for many biomedical and pharmaceutical applications. For example,

CH-microspheres have been used as carriers for controlled release of drugs, peptides and proteins, as well as vaccines.<sup>2-4</sup> The modulation of drug release rate from CH-microspheres had been obtained by matrix cross-linking. This made the polymer less hydrophilic and slowed down the permeability to biological fluids. In fact, the cross-linking process can be performed by using chemical substances acting as cross-

linking agents, or by heating. The most often used chemical cross-linkers for microspheres made of the natural polymers are glutaraldehyde and epichlorohydrin. Of the former, it acts on the polymer by dissolving it in one of the liquid phase, while the later has been used to cross-link CH-fibers and films.<sup>3,5</sup> The main disadvantages of both cross-linking agents are skin irritation and exerting some toxicity. When heat is applied as cross-linking agent, the formed microspheres must be exposed to a longer time period at high temperature about 120°C or more. Therefore, drug instability is a major problem of thermal cross-linking. Another cross-linking mechanism, such as ionic interaction, can be employed to overcome toxicity of chemical cross-linking. Since CH becomes soluble and cationic in aqueous acidic solutions of pH<6.5, tripolyphosphate (TPP), a nontoxic salt obtained from triple condensation of  $\text{PO}_4^{3-}$  groups, can interact with protonated amino groups of CH, forming insoluble complexes with raise medium pH.<sup>3,6</sup> Increased drug loading efficiency and prolonged drug release period have been revealed by these complexes as well.<sup>7,8</sup> They have been successfully prepared by a number of methods, such as simple/complex coacervation<sup>9</sup> and freeze-drying.<sup>4</sup>

Nowadays, ceramics as comprised of calcium phosphates, silica, alumina, zirconia and titanium dioxide are used for various medical applications due to their positive interactions with human tissues.<sup>10</sup> Characteristics of these materials are often high mechanical strength, good body-response and low or non-existing biodegradability. Due to their similarity to human bone, calcium phosphate ceramics are very popular implant materials for diverse clinical applications since the last 30 years. Especially, hydroxyapatite (HA) is regarded as a high potential scaffold because of its osteoconductive and osteoinductive properties.<sup>11,12</sup> To improve the biodegradability, porosity has been introduced to the implants, which also gives rise to bone ingrowth.<sup>13,14</sup> Although ceramic scaffolds alone can be suitable implant materials for bone tissue engineering, they can form a suitable scaffold for cells and serve as a delivery vehicle of drugs by the addition of biodegradable polymers. Of these polymers, CH is often applied together with calcium phosphate particles because it is degraded by endogenous enzymes and gives a good match to natural bone with respect to mechanical properties. The added ceramic particles gave scaffolds an extra osteogenic potential, while the composite materials showed enhanced osteoblast proliferation and differentiation.<sup>15</sup> Moreover, release patterns of the scaffolds loaded with gentamycin showed a high burst release, which was diminished by the added ceramic particles. Indeed, a more sustained release from the particle-containing CH-composite was observed to be due to a higher extent of CH cross-linking.<sup>16</sup>

The goal of this work was to develop a convenient method for preparing beads of HA/CH composite cross-linked by ionic interaction of TPP for controlled release of TCH. Some problems arose when TCH was impregnated into the particle-

polymer composite prior to perform cross-linking, because the drug has high solubility in aqueous acidic solvent used for dissolving CH. This led to the loss of large amounts of drug during the preparation process. In consequence, cross-linked HA/CH beads were firstly prepared and then soaked in a solution containing TCH under vacuum. In estimation, the amount of drug adsorbed onto the bead would be influenced by factors such as the drug concentration, drug binding moieties, matrix porosity, and cross-linking density. Besides, the degree of cross-linking and swelling would affect the drug release pattern. Thus, experiments were conducted in this study to gain insight into parameters which are influenced by cross-linking density of the HA/CH beads.

## 2.0 Materials and Methods

### 2.1 Preparation of HA/CH beads

Different CH solutions were prepared by dissolving CH in 3% aqueous acetic acid in a beaker with a magnetic stirrer. One hundred milliliters of the solution were levigated with distinct amounts of HA to form smooth paste. HA/CH beads were formed as drops of the mixed paste fell into a precipitation bath containing TPP solution in which its concentrations were varied between 0.5 and 1% w/v. TPP cross-linking was allowed to form for 24 h at room temperature. After that the beads were rinsed several times with water and then freeze-dried. The cross-linked beads were manipulated using quantitatively specified compositions as summarized in Table 1.

Chemical used				
Chitosan solution <sup>1</sup> (% w/v)	HA (g)	TPP solution <sup>2</sup> (% w/v)	Ratio by mass of CH:HA:TPP	Name assigned
1	20	0.7	1:20:2.1	TPPex
1.5	30	1	1:20:2	TPPeq
1.5	40	1	1:20.6:2	HAex

<sup>1</sup> and <sup>2</sup> were the solutions used at a fixed volume of 100 and 300 ml, respectively

### 2.2 Scanning electron microscope (SEM)

Scanning electron microscopy (SEM, FEI Quanta 400) was carried out for visual inspection of surface morphology and cross-sectional structure of the drug-free beads. Samples were mounted on metal stubs using double-side adhesive tape and vacuum-coated with gold film. Porosity and pore size inside the beads were estimated from ten data points of triple SEM micrographs.

### 2.3 Infrared absorption spectroscopy (IR)

Each sample was triturated with an equal quantity of KBr and compressed to obtain a disc for IR analysis. The spectra of the discs were recorded on a FTIR spectrophotometer (Spectrum One, Perkin Elmer, USA) in a region between 500 and 4000  $\text{cm}^{-1}$ . The experiments were carried out in triplicate.

## 2.4 Acellular *in vitro* bioactivity

Phosphate buffer saline (PBS) pH 7.4<sup>17</sup> containing HA/CH beads without drug loading in a well-closed polystyrene bottle was maintained at 37 °C. Samples were collected after 7 days of the immersion and analyzed by SEM.

## 2.5 Swelling study

The degree of swelling (DW) was used to correlate release characteristics of TCH from HA/CH beads in this study. Briefly, an accurately weighed amount of dried samples was placed in a 10-ml reservoir containing PBS pH 7.4 without shaking at 37 °C. The weight of each swollen sample (Wt) was determined on an electronic balance following the soaked solution was blotted out. DS was expressed as the percentage of water absorbed at any time during swelling, and calculated by the equation as followed:

$$\% \text{ DS} = [(W2 - W1) \div W1] \times 100$$

W1 and W2 represented the weight of dry HA/CH beads and that of wet samples, respectively.

## 2.6 Preparation of drug-loaded HA/CH beads

TCH was dissolved in water to achieve concentrations in a range of 5-15 mg/ml. The beads were loaded with TCH by vacuum infiltration method. In brief, an accurately weighed amount of the beads was placed in a tube containing 5 ml of TCH solution. Then, a vacuum of 0.1 ton/inch<sup>2</sup> was applied for 30 min. After vacuum was released, the drug-loaded beads were freeze-dried and kept at -15 °C until use.

## 2.7 Drug entrapment

An accurately weighed amount of drug-loaded beads were crushed and kept under constant stirring in diluted hydrochloric acid (10% v/v) for 20 min to extract TCH from the bead matrix. After centrifugation, the supernatant was determined spectrophotometrically at 270 nm. For calculating the amounts of TCH adsorbed, the measured OD was compared to the standard  $A_{1\%, 1\text{ cm}}$  at 270 nm of 417a. Then, the entrapment efficiency (EE) was indicated as milligrams of the drug adsorbed per gram of the bead sample.

## 2.8 Drug release *in vitro*

To determine the quantity of TCH released from the beads, an accurately weighed sample was set into a tube containing 5 ml

of PBS pH 7.4 at 37 °C for a period of 7 days. One milliliter of the supernatant was withdrawn at a predetermined time interval and replaced by an equal volume of fresh medium. The collected solutions were measured for OD at 270 nm in which the drug concentrations were calculated by comparing with the standard  $A_{1\%, 1\text{ cm}}$  as previously described. The cumulative percentage of drug release was represented after being normalized to its initial amount in the beads.

## 2.9 Statistical analysis

All data were expressed as mean  $\pm$  S.D. of an experiment carried out in triplicate. Student's *t*-test (Sigma Plot) with  $P < 0.05$  was used to determine the significant differences between the groups.

## 3.0 Results and Discussion

Sustained drug release technology is being applied from protein hormones such as insulin for the treatment of diabetes<sup>18</sup> to antibiotics for the prevention or minimization of bacterial infection.<sup>19,20</sup> Advantages of this technology are associated with reduction in side effects, decreased systemic toxicity and higher efficiency due to high drug concentrations at the site of damage.<sup>21</sup> Improvements on the field are based on the development of new biocompatible synthetic<sup>22</sup> and natural polymers<sup>23</sup> and bioceramic.<sup>24</sup> Among the natural polymers, CH has been an attractive candidate for drug delivery matrix due to its high biocompatibility, low antigenicity, controlled biodegradability by cross-linking reagents, and the ease of forming composites with ceramics or synthetic polymers.<sup>2,3,25</sup>

In our preliminary study, the HA/CH beads encapsulating TCH were prepared by the impregnation process in that the TCH/HA blend was levigated with CH solution, followed by TPP cross-linking. Although the drug was dispersed uniformly in the polymeric monolithic system, the percentage of drug entrapment was very low (less than 4%). By duplicating the amount of drug in the loading process, however, improvement in the encapsulation efficiency was not apparent. As a result, drug loss during the preparation process was large. This might be due to the high porosity of the beads, associated with a high solubility in water of the drug in the form of hydrochloride salt. In fact, beads prepared by the impregnation method should be rigid and contain pores able to hold substances inside by capillary forces, while allow full diffusion outward of the retained active ingredient.<sup>26</sup> In consequence, the infiltration method was adopted in this study to encapsulate TCH in cross-linked CH/HA beads, followed by the determination of the cross-linking density affecting on %DS and drug release.

## 3.1 Morphology of cross-linked HA/CH beads

The mixed composite paste of HA and CH had a good shape-forming ability in TPP cross-linking solution. The beads also displayed a uniform round shape after the freeze-drying process. However, obvious deformation in the final structure had occurred if the bead compositions were not optimal (Figure 1). The cross-sectional SEM morphologies of HA/CH beads without drug loading were shown in Figures 2. A well developed porous structure consisting of open pore channels and an interconnected framework was observed. Most of these pores were of irregular shape with an average pore diameter of about  $45 \pm 17 \mu\text{m}$ . The pore size was further decreased by increasing HA content. The pores were predominantly in the range suitable for drug delivery applications, as small pores facilitated high absorption of drug and sustained the release better than the larger pores.<sup>27,28</sup> SEM images of the TPPEq beads subjected to acellular *in vitro* bioactivity study were presented in Figure 3. The bead structure was intact for the entire period of 7 days in PBS. After soaking, significant change on the surfaces was demonstrated in that deposits appearing as much bigger agglomerates of fur stacked on one another. Interestingly, pores in micrometer range were still visible on the immersed surfaces. Since the ability to deposit apatite on the material surface *in vitro* implies biological response following a series of physiological reactions at the material–biological site interface<sup>15</sup>, the result suggested that this type of beads was attractive as a drug carrier to bone.

### 3.2 FTIR analysis

The phase compositions of HA/CH beads were investigated using FTIR spectroscopy. According to the literature, FTIR spectrum of CH showed peaks at  $1089$  and  $1152 \text{ cm}^{-1}$  for aliphatic amines and at  $1650 \text{ cm}^{-1}$  for N-H group (Figure 4A). Especially determined in the spectra of TPPEq and HAex (Figure 4B and insert), peaks at  $1060\text{--}1300 \text{ cm}^{-1}$  were of phosphonate linkages occurring between  $\text{--NH}^{3+}$  of CH and  $\text{--PO}_4^{3-}$  moieties of TPP during the cross-linking process.

Appreciable cross-linking was revealed by peaks at  $1140$  and  $1280 \text{ cm}^{-1}$ , indicative for symmetric and asymmetric stretching of phosphonate linkage, respectively. The latter peak has been known to occur due to restricted rotation.<sup>29</sup> Therefore, the two terminal  $\text{--PO}_4^{3-}$  moieties of a TPP molecule seemed to link with two  $\text{--NH}_3^+(\text{OOCCH}_3)\text{--}$  moieties of two CH monomers, one on each side. This cross-linking perhaps restricted the permeation of drug molecules and lowered the flux of drug diffusing across the beads. However, the asymmetric peak trended to merge into a single broad band at  $1060 \text{ cm}^{-1}$ , as seen in the spectrum of TPPex. The result indicated the absence of restricted rotation within the beads cross-linked by using excess TPP. The excessive  $\text{--PO}_4^{3-}$  moieties of TPP were also confirmed by a triplet broad peak detected around  $640 \text{ cm}^{-1}$ . In consequence, greater permeation of the drug was observed across the TPPex beads (data not shown).



Fig.1 Photographs of HA/CH composite beads: (A), TPPex; (B), TPPEq; (C), HAex

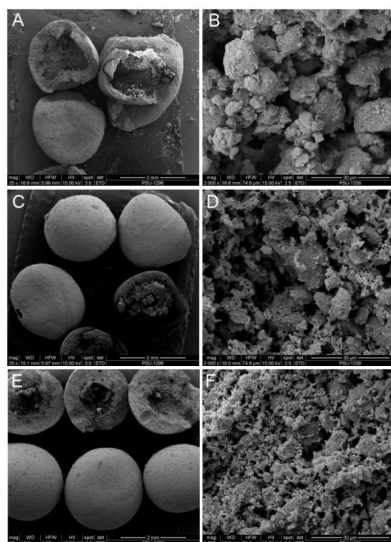


Fig. 2 SEM micrographs of HA/CH composite beads and their cross-sections: (A and B),

### 3.3 Swelling result

The *in vitro* swelling study was conducted in PBS pH 7.4 at  $37^\circ\text{C}$  for a period of 7 days, and the %DS was gravimetrically determined. Plots of static swelling of the cross-linked beads as a function of TPP concentrations were given in Figure 5. It was found that all cross-linked structures were hydrolytically stable. Greater swelling was observed for TPPex due to the more loosely structure. The close similarity of %DS was determined for TPPEq and HAex beads. It would be that as the degree of cross-linking was optimal, ionic interactions became predominant resulting in the more compact structure of the later two samples. The influence of ionic interactions between chains of CH in the beads on swelling has been reported to depend on the cross-linking density achieved during the formation of the network, i.e., an increase in cross-linking density induced a decrease of swelling.<sup>3</sup> In estimation, the swelling mechanism has involved



structure relaxation due to dissociation of hydrogen bridges and hydrophobic interactions occurring between acetylated units of CH, followed by swelling.

### 3.4 Drug entrapment and release behavior

Based on the swelling test, the bead of much higher intact structure was identified for HAex. In consequence, they were used thoroughly for drug entrapment and release test.

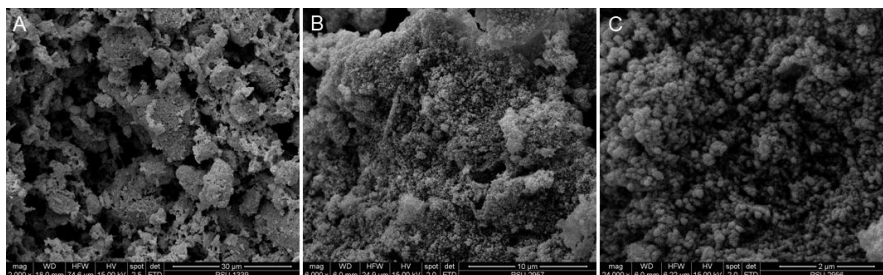


**Fig. 3** SEM images of TPPEq beads before (A), after immersed in PBS for 7 days at low (B) and high (C) magnification

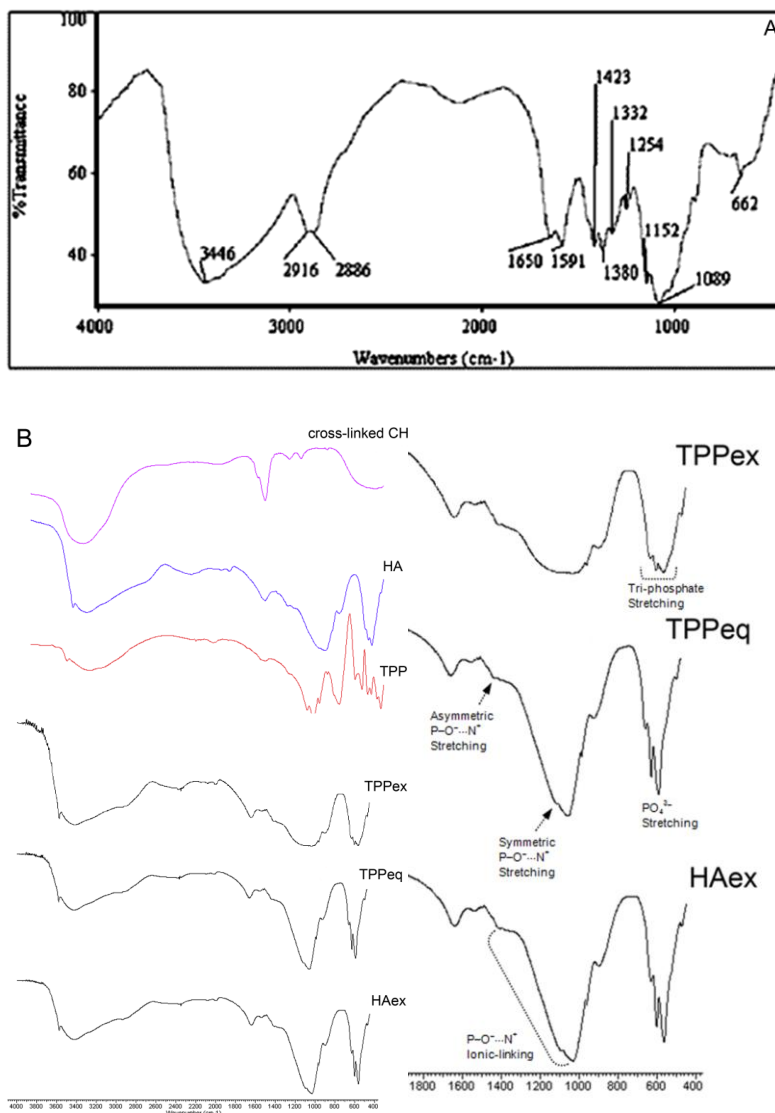


**Fig. 4** FTIR spectra of unmodified CH powder (A), CH (1% w/v) films cross-linked with 1% w/v TPP (B, on top), and HA/CH composite beads of TPPEq, TPPEq, as well as HAex (B, three spectra in bottom), relevant regions are indicated in the insert figure, as detailed in text

Three concentration levels of TCH solutions were used during the infiltration process (5, 10, and 15 mg/ml) in which the EE values were calculated to be of 17.7, 28.7, and 32.2 mg/g, respectively. By investigating the effect of drug content on release pattern, it revealed that all of the beads displayed a long period of sustained release without an initial burst (Figure 6A). On the first day of the test, about 20% of the entrapped TCH was released from the beads (Figure 6B).

During a follow-up period of 6 days, drug release continued at a much slower release rate, supposing to be via diffusion of the entrapped drug through the porous network. The release test was not carried out after 7 days, because of the drug instability problem. Moreover, the association between %HA and the pore size on TCH release rate was investigated. The release rate was found to decrease, proportional to the decrease in pore size of the beads by increasing %HA (data not shown).

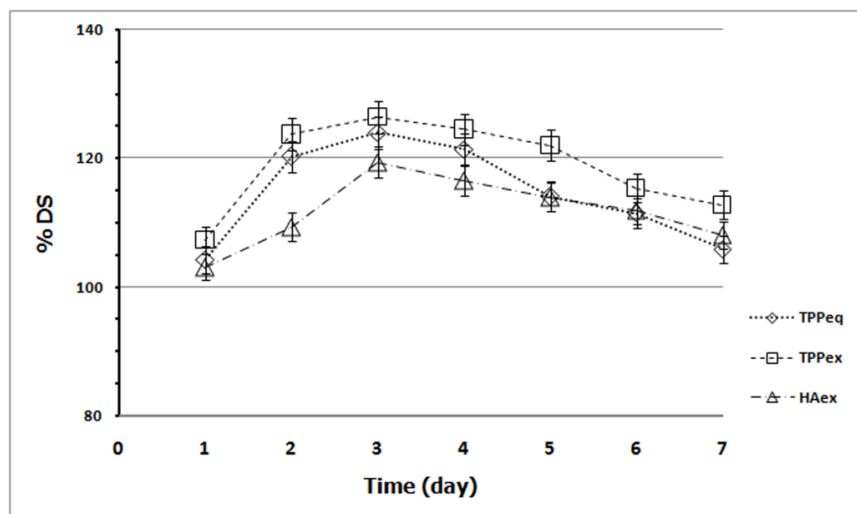


Fig. 5 Swelling behavior of HA/CH composite beads (TPPex, TPPeq, and HAex), cross-linked with various concentrations of TPP

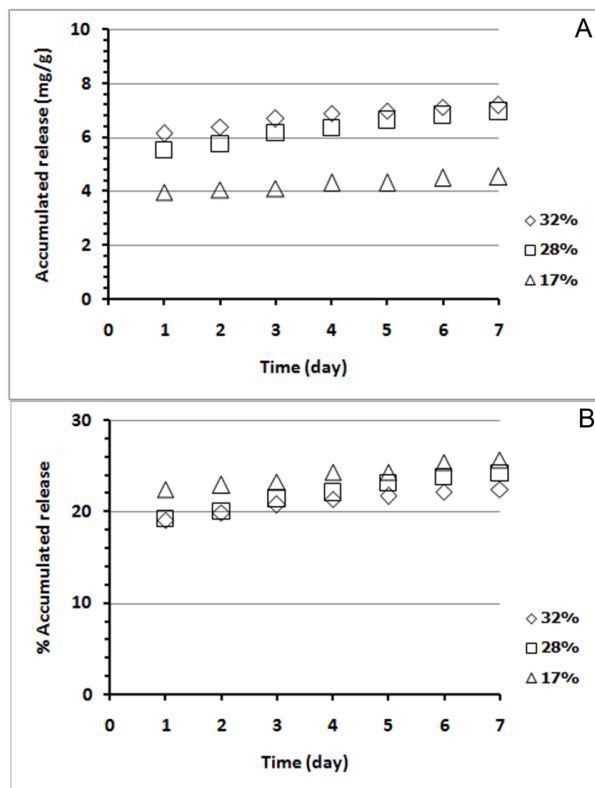


Fig. 6 Drug release patterns of HA/CH composite beads with a fixed %HA, indicating the effect of concentration of drug in loading solution on drug release.

In concomitance, the lower porosity and the lower degree of swelling of HAex beads led to TCH being more difficultly diffusing. In contrast to TPPex beads which had the higher degree of swelling, the access of medium to the drug incorporated in the polymeric matrix was facilitated, consequently increasing contact with it and allowing greater release. In spite of the higher porosity and the higher TCH entrapment of TPPex beads, the drug release was not different from those previously mentioned. This was because the difference in %DS could not be significantly assigned among the prepared beads, making similar entry of the medium into the polymer matrix. Thus, increase in the rates of drug release could be due to an associated increase in the fluid-filled cavities created by swelling, dissolution and diffusion of the drug particles near the surface. This in turn resulted in an increase of the permeability of the drug. However, release of substances has been described to depend on the type of matrix and its rigidity, i.e., the release of drugs decreased with increased cross-linking.<sup>25</sup> Indeed, factors such as the cross-linking density and porosity, the degree of swelling, as well as drug solubility have been determinants controlling the release of substances from cross-linked network.<sup>26</sup> Notably, a considerable fraction of drug molecules was attached to the pore surface, as the entrapped drug was released in the range of 20-24% within 7 days.

This drug fraction was probably bound to the beads via hydrogen bonding between the highly electronegative atoms/groups such as N and OH of the drug and P–OH groups of HA, or absorbed onto the HA particles due to its strong affinity with calcium ions.<sup>30</sup> It was proposed that the remaining drug would only be released in concomitance with slow degradation of the beads. However, the release concentrations were significantly higher than that described for the prevention of bacterial growth.<sup>31</sup> In summary; this study presented a simple but efficient method to prepare beads of TCH-entrapped HA/CH composite with a porous structure. The macro- and micro-pores of the beads formed during the cross-linking and freeze-drying processes facilitated their use in delivery of drugs or bioactive molecules for enhanced tissue regeneration of bone.

## Acknowledgement

Financial support for this work was obtained from Prince of Songkla University through the Discipline of Excellence in Chemical Engineering, Department of Chemical Engineering, Faculty of Engineering; and Drug Delivery System Excellence Center, Faculty of Pharmaceutical Sciences.

## References

1. Kumar MNVR. A review of chitin and chitosan applications. *React Funct Polym.* 2000;46:1-27.
2. Sinha VR, Singla AK, Wadhawan S, Kaushik R, Kumria R, Bansal, K., Dhawan, S. Chitosan microspheres as a potential carrier for drugs. *Int J Pharm.* 2004;274:1-33.
3. Mi FL, Shyu SS, Chen CT, Schoung JY. Porous chitosan microsphere for controlling the antigen release of Newcastle disease vaccine: preparation of antigen-adsorbed microsphere and in vitro release. *Biomaterials* 1999;20:1603-1612.
4. Calvo P, Remuñá-López C, Vila-Jata JL, Alonso MJ. Novel hydrophilic chitosan-propylene glycol oxide nanoparticles as protein carriers. *J Appl Polym Sci.* 1997;63:125-132.
5. Blanco MD, Gómez C, Olmo R, Muñiz E, Tejiño JM. Chitosan microspheres in PLG films as devices for cytarabine release. *Int J Pharm.* 2000;202:29-39.
6. Aral C, Akugba J. Alternative approach to the preparation of chitosan beads. *Int J Pharm.* 1998;168:9-15.
7. Van der Lubben IM, Kersten G, Fretz MM, Beuvery C, Verhoef JC, Junginger HE. Chitosan microparticles for mucosal vaccination against diphtheria: oral and nasal efficacy studies in mice. *Vaccine* 2003;21:1400-1408.
8. Xu Y, Du Y. Effect of molecular structure of chitosan on protein delivery properties of chitosan nanoparticles. *Int J Pharm.* 2003;250:215-226.
9. Yao K, Peng T, Yin Y, Xu M, Goosen MFA. Microcapsules/microspheres related to chitosan. *JMS Rev Macromol Chem Phys.* 1995;C35:155-180.
10. Barsoum MW. Fundamentals of ceramics, in: Gibala R, Tirrell M, West CA (Eds.), *McGraw-Hill Series in Materials Science and Engineering: The McGraw-Hill Companies, Inc;* 1997:2.
11. Kenny SM, Buggy M. Bone cements and fillers: a review. *J Mater Sci Mater Med.* 2003;14: 923–938.
12. Thomas MV, Puleo DA, Al-Sabbagh M. Bioactive glass three decades on. *J Long-Term Effect Med Implants* 2005;15:585–597.
13. Habibovic P, Sees TM, van den Doel MA, van Blitterswijk CA, de Groot K. Osteoinduction by biomaterials Physicochemical and structural influences. *J Biomed Mater Res.* 2006;A77:747–762.
14. Karageorgiou V, Kaplan D. Porosity of 3D biomaterial scaffolds and osteogenesis. *Biomaterials* 2005;26:5474–5491.
15. Habraken WJEM, Wolke JGC, Jansen JA. Ceramic composites as matrices and scaffolds for drug delivery in tissue engineering. *Adv Drug Delivery Rev.* 2007;59:234–248.
16. Lee YM, Park YJ, Lee SJ, Ku Y, Han SB, Klokkevoeld PR, Chung CP. The bone regenerative effect of platelet-derived growth factor-BB delivered with a chitosan/tricalcium phosphate sponge carrier. *J Periodontol.* 2000;71:418–424.
17. Sambrook J, Fritsch EF, Maniatis T. *Molecular Cloning: A Laboratory Manual*, 2nd ed. New York: Harbor Laboratory Press, Cold Spring Harbor; 1989.
18. Obaidat AA, Park K. Characterization of protein release through glucose-sensitive hydrogel membranes. *Biomaterials* 1997;18:801-806.
19. Kwok CS, Horbett TA, Ratner BD. Design of infection-resistant antibiotic-releasing polymers, II. Controlled release of antibiotics through a plasma-deposited thin film barrier. *J Contr Rel.* 1999;62:301-311.
20. Meyer JD, Falk RF, Kelly RM, Shively JE, Withrow SJ, Dernel WS, Kroll DJ, Randolph TW, Manning MC. Preparation and in vitro characterization of gentamicin-

impregnated biodegradable beads suitable for treatment of osteomyelitis. *J Pharm Sci.* 1998;87:1149-1154.

21. Dash AK, Cudworth GC. Therapeutic applications of implantable drug delivery systems. *J Pharmacol Toxicol Methods* 1998;40:1-12.

22. Schierholz JM, Steinhauser H, Rump AF, Berkels R, Pulverer G. Controlled release of antibiotics from biomedical polyurethane: morphological and structural features. *Biomaterials* 1997;18:839-844.

23. Hari PR, Chandy T, Sharma CP. Chitosan/calcium alginate microcapsules for intestinal delivery of nitrofurantoin. *J Microencapsul.* 1996;13:319-329.

24. Itokazu M, Ohno T, Tanemori T, Wada E, Kato N, Watanabe K. Antibiotic-loaded hydroxyapatite blocks in the treatment of experimental osteomyelitis in rats. *J Med Microbiol.* 1997;46:779-783.

25. Kumbar SG, Kulkarni AR, Aminabhvi TM. Crosslinked chitosan microspheres for encapsulation of diclofenac sodium: effect of crosslinking agent. *J Microencapsul.* 2002;19:173-180.

26. Teng SH, Lee EJ, Wang P, Jun SH, Han CM, Kim HE. Functionally Gradient Chitosan/Hydroxyapatite Composite Scaffolds for Controlled Drug Release. Published online 11 December 2008 in Wiley InterScience: DOI: 10.1002/jbm.b.31283

27. Soundrapandian C, Datta S, Sa B. Drug-eluting implants for osteomyelitis. *Crit Rev Ther Drug Carrier Syst.* 2007;24:493-545.

28. Seeley Z, Bandyopadhyay A, Bose S. Tricalcium phosphate based resorbable ceramics: Influence of NaF and CaO addition. *Mater SciEng C.* 2008;28:11-17.

29. Kemp W. *Infrared Spectroscopy*, London: Macmillan Press; 1991:19-56.

30. Ratier A, Freche M, Lacout JL, Rodriguez F. Behavior of an injectable calcium phosphate cement with added tetracycline. *Int J Pharm.* 2004;274:261–268.

31. Klajn R. Chemistry and chemical biology of tetracyclines. (<http://www.chm.bris.ac.uk/motm/tetracycline/antimicr.htm>)